BELLE-CONF-0004
Parallel Session: PA-07e
Plenary Session: PL-01b

Observation of $B \to J/\psi K_1(1270)$

Belle Collaboration

Abstract

We report the first observation of the exclusive decay $B \to J/\psi K_1(1270)$ in the Belle detector at the KEKB collider. Preliminary results for $B^+ \to J/\psi K_1^+(1270)$ and $B^0 \to J/\psi K_1^0(1270)$ branching fractions are given. Implications for indirect CP violation measurements are discussed.

Typeset using REVTEX

A. Abashian[44], K. Abe[8], K. Abe[36], I. Adachi[8], Byoung Sup Ahn[14], H. Aihara[37], M. Akatsu[19], G. Alimonti[7], K. Aoki[8], K. Asai[20], M. Asai[9], Y. Asano[42], T. Aso[41], V. Aulchenko[2], T. Aushev[12], A. M. Bakich[33], E. Banas[15], S. Behari[8], P. K. Behera[43], D. Beiline[2], A. Bondar[2], A. Bozek[15], T. E. Browder[7], B. C. K. Casey[7], P. Chang[23], Y. Chao[23], B. G. Cheon[32], S.-K. Choi[6], Y. Choi[32], Y. Doi[8], J. Dragic[17], A. Drutskoy[12], S. Eidelman[2], Y. Enari[19], R. Enomoto[8,10], C. W. Everton[17], F. Fang[7], H. Fujii[8], K. Fujimoto[19], Y. Fujita[8], C. Fukunaga[39], M. Fukushima[10], A. Garmash[2,8], A. Gordon[17], K. Gotow[44], H. Guler[7], R. Guo[21], J. Haba[8], T. Haji[4], H. Hamasaki[8], K. Hanagaki[29], F. Handa[36], K. Hara[27], T. Hara[27], T. Haruyama[8], N. C. Hastings[17], K. Hayashi[8], H. Hayashii[20], M. Hazumi[27], E. M. Heenan[17], Y. Higashi[8], Y. Higasino[19], I. Higuchi[36], T. Higuchi[37], T. Hirai[38], H. Hirano[40], M. Hirose[19], T. Hojo[27], Y. Hoshi[35], K. Hoshina[40], W.-S. Hou[23], S.-C. Hsu[23], H.-C. Huang[23], Y.-C. Huang[21], S. Ichizawa[38], Y. Igarashi[8], T. Iijima[8], H. Ikeda[8], K. Ikeda[20], K. Inami[19], Y. Inoue[26], A. Ishikawa[19], R. Itoh[8], G. Iwai[25], M. Iwai[8], H. Iwasaki[8], Y. Iwasaki[8], D. J. Jackson[27], P. Jalocha[15], H. K. Jang[31], M. Jones[7], R. Kagan[12], H. Kakuno[38], J. Kaneko[38], J. H. Kang[45], J. S. Kang[14], P. Kapusta[15], K. Kasami[8], N. Katayama[8], H. Kawai[3], M. Kawai[8], N. Kawamura[1], T. Kawasaki[25], H. Kichimi[8], D. W. Kim[32], Heejong Kim[45], H. J. Kim[45], Hyunwoo Kim[14], S. K. Kim[31], K. Kinoshita[5], S. Kobayashi[30], S. Koike[8], Y. Kondo[8], H. Konishi[40], K. Korotushenko[29], P. Krokovny[2], R. Kulasiri[5], S. Kumar[28], T. Kuniya[30], E. Kurihara[3], A. Kuzmin[2], Y.-J. Kwon[45], M. H. Lee[8], S. H. Lee[31], C. Leonidopoulos[29], H.-B. Li[11], R.-S. Lu[23], Y. Makida[8], A. Manabe[8], D. Marlow[29], T. Matsubara[37], T. Matsuda[8], S. Matsui[19], S. Matsumoto[4], T. Matsumoto[19], K. Misono[19], K. Miyabayashi[20], H. Miyake[27], H. Miyata[25], L. C. Moffitt[17], G. R. Moloney[17], G. F. Moorhead[17], N. Morgan[44], S. Mori[42], T. Mori[4], A. Murakami[30], T. Nagamine[36], Y. Nagasaka[18], Y. Nagashima[27], T. Nakadaira[37], T. Nakamura[38], E. Nakano[26], M. Nakao[8], H. Nakazawa[4], J. W. Nam[32], S. Narita[36], Z. Natkaniec[15], K. Neichi[35], S. Nishida[16], O. Nitoh[40], S. Noguchi[20], T. Nozaki[8], S. Ogawa[34], R. Ohkubo[8], T. Ohshima[19], Y. Ohshima[38], T. Okabe[19], T. Okazaki[20], S. Okuno[13], S. L. Olsen[7], W. Ostrowicz[15], H. Ozaki[8], P. Pakhlov[12], H. Palka[15], C. S. Park[31], C. W. Park[14], H. Park[14], L. S. Peak[33], M. Peters[7], L. E. Piilonen[44], E. Prebys[29], J. Raaf[5], J. L. Rodriguez[7], N. Root[2], M. Rozanska[15], K. Rybicki[15], J. Ryuko[27], H. Sagawa[8], Y. Sakai[8], H. Sakamoto[16], H. Sakaue[26], M. Satapathy[43], N. Sato[8], A. Satpathy[8,5], S. Schrenk[44], S. Semenov[12], Y. Settai[4], M. E. Sevior[17], H. Shibuya[34], B. Shwartz[2], A. Sidorov[2], V. Sidorov[2], S. Stanič[42], A. Sugi[19], A. Sugiyama[19], K. Sumisawa[27], T. Sumiyoshi[8], J. Suzuki[8], J.-I. Suzuki[8], K. Suzuki[3], S. Suzuki[19], S. Y. Suzuki[8], S. K. Swain[7], H. Tajima[37], T. Takahashi[26], F. Takasaki[8], M. Takita[27], K. Tamai[8], N. Tamura[25], J. Tanaka[37], M. Tanaka[8], Y. Tanaka[18], G. N. Taylor[17], Y. Teramoto[26], M. Tomoto[19], T. Tomura[37], S. N. Tovey[17], K. Trabelsi[7], T. Tsuboyama[8], Y. Tsujita[42], T. Tsukamoto[8], T. Tsukamoto[30], S. Uehara[8], K. Ueno[23], N. Ujiie[8], Y. Unno[3], S. Uno[8], Y. Ushiroda[16], Y. Usov[2], S. E. Vahsen[29], G. Varner[7], K. E. Varvell[33], C. C. Wang[23], C. H. Wang[22], M.-Z. Wang[23], T.-J. Wang[11], Y. Watanabe[38], E. Won[31], B. D. Yabsley[8], Y. Yamada[8], M. Yamaga[36], A. Yamaguchi[36], H. Yamaguchi[8], H. Yamamoto[7], H. Yamaoka[8], Y. Yamaoka[8], Y. Yamashita[24], M. Yamauchi[8], S. Yanaka[38], M. Yokoyama[37], K. Yoshida[19], Y. Yusa[36], H. Yuta[1], C.-C. Zhang[11], H. W. Zhao[8], Y. Zheng[7], V. Zhilich[2], and D. Žontar[42]

[1]Aomori University, Aomori

[2]Budker Institute of Nuclear Physics, Novosibirsk
[3]Chiba University, Chiba
[4]Chuo University, Tokyo
[5]University of Cincinnati, Cincinnati, OH
[6]Gyeongsang National University, Chinju
[7]University of Hawaii, Honolulu HI
[8]High Energy Accelerator Research Organization (KEK), Tsukuba
[9]Hiroshima Institute of Technology, Hiroshima
[10]Institute for Cosmic Ray Research, University of Tokyo, Tokyo
[11]Institute of High Energy Physics, Chinese Academy of Sciences, Beijing
[12]Institute for Theoretical and Experimental Physics, Moscow
[13]Kanagawa University, Yokohama
[14]Korea University, Seoul
[15]H. Niewodniczanski Institute of Nuclear Physics, Krakow
[16]Kyoto University, Kyoto
[17]University of Melbourne, Victoria
[18]Nagasaki Institute of Applied Science, Nagasaki
[19]Nagoya University, Nagoya
[20]Nara Women's University, Nara
[21]National Kaohsiung Normal University, Kaohsiung
[22]National Lien-Ho Institute of Technology, Miao Li
[23]National Taiwan University, Taipei
[24]Nihon Dental College, Niigata
[25]Niigata University, Niigata
[26]Osaka City University, Osaka
[27]Osaka University, Osaka
[28]Panjab University, Chandigarh
[29]Princeton University, Princeton NJ
[30]Saga University, Saga
[31]Seoul National University, Seoul
[32]Sungkyunkwan University, Suwon
[33]University of Sydney, Sydney NSW
[34]Toho University, Funabashi
[35]Tohoku Gakuin University, Tagajo
[36]Tohoku University, Sendai
[37]University of Tokyo, Tokyo
[38]Tokyo Institute of Technology, Tokyo
[39]Tokyo Metropolitan University, Tokyo
[40]Tokyo University of Agriculture and Technology, Tokyo
[41]Toyama National College of Maritime Technology, Toyama
[42]University of Tsukuba, Tsukuba
[43]Utkal University, Bhubaneswer
[44]Virginia Polytechnic Institute and State University, Blacksburg VA
[45]Yonsei University, Seoul

I. INTRODUCTION

Decays of B mesons into final states containing the J/ψ charmonium state play a special role in studies of CP violation physics. Since the J/ψ is itself a CP eigenstate, final states where the accompanying particles are matter-antimatter symmetric are potentially useful for studying CP-violations. Moreover, these decay modes are experimentally convenient, primarily because the $J/\psi \to \ell^+\ell^-$ ($\ell^+\ell^- = e^+e^-$ or $\mu^+\mu^-$) final states have a rather distinct experimental signature.

However, although the inclusive branching fraction for $B \to J/\psi X$ is relatively large ($\sim 1\%$), only a small fraction of these decays have been associated with exclusive decay modes that are relevant for CP violation studies. Since all current experimental searches for CP violations in B meson decays are statistics limited, it is of considerable interest to identify additional decay modes that might be useful. Decays of the type $B^0 \to J/\psi K_1^0(1270)$ would be of special interest because the $K_1(1270)$ has an appreciable branching fraction to the *flavor-nonspecific* $K^0\rho^0$ final state (14%). However, at present there is very little experimental information available about any exclusive $B \to J/\psi K\pi\pi$ decay modes [1].

In this report we describe a study of the $B \to J/\psi K\pi\pi$ decay process using the Belle detector at the KEKB asymmetric energy e^+e^- storage ring [2]. We observe a signal for exclusive decays where the $K\pi\pi$ system has the properties of the $K_1(1270)$ resonance. The data sample corresponds to an integrated luminosity of approximately 5.3 fb^{-1}, accumulated at the $\Upsilon(4S)$ resonance.

II. THE BELLE DETECTOR

Belle is a large-solid-angle spectrometer based on a 1.5 Tesla superconducting solenoid magnet. Charged particle tracking is provided by a silicon vertex detector (SVD) and a cylindrical drift chamber (CDC) that surround the interaction region. The SVD consists of three layers of double-sided silicon strip detectors; one side measures the z and the other the $r-\phi$ coordinate [3]. The CDC has 50 cylindrical layers of anode wires; the inner three layers have instrumented cathodes for z coordinate measurements [4]. Twenty of the wire layers are inclined at small angles to provide small-angle-stereo z coordinates measurements at larger radii. The charged particle acceptance covers the laboratory polar angle region between $\theta = 17^o$ and 150^o, corresponding to about 92% of the full cm solid angle.

Tracks are fit using an incremental Kalman filtering technique, where individual measurements found by the CDC pattern recognition algorithm are added successively to update the track's parameters and covariance matrix at each measurement surface. This approach to track fitting minimizes the effects of multiple Coulomb scattering on the determination of the track parameters. Hits from the SVD hits are associated and included during the last steps of this recursion. The momentum resolution is determined from cosmic rays and $e^+e^- \to \mu^+\mu^-$ events to be $\sigma_{p_t}/p_t = (0.36 \oplus 0.28 p_t)\%$, where p_t is the transverse momentum in GeV.

Charged hadron identification is provided by dE/dx measurements in the CDC, a mosaic array of 1188 aerogel Čerenkov counters (ACC), and a barrel of 128 time-of-flight scintillation counters (TOF). The dE/dx measurements have a resolution for hadron tracks of 6.9% and are useful for π/K separation for $p_{lab} < 0.8$ GeV and $p_{lab} > 2.5$ GeV, where p_{lab}

is the laboratory momentum. The TOF system has a time resolution for hadrons that is $\sigma \simeq 100$ ps and provides π/K separation for $p_{lab} < 1.5$ GeV [5]. The indices of refraction of the ACC elements vary with polar angle to match the kinematics of the asymmetric energy environment of Belle and cover the range $1.5 < p_{lab} < 3.5$ GeV [6]. Particle identification probabilities are determined from the combined response of the three systems. High momentum tagged kaons and pions derived from kinematically selected $D^{*+} \to D^0\pi^+$; $D^0 \to K^-\pi^+$ decays are used to determine a charged particle identification efficiency of 80% and a misidentification probability of 8%.

Electromagnetic showering particles are detected in an array of 8736 CsI crystals that covers the same solid angle as the charged particle tracking system [7]. The energy resolution for electromagnetic showers is $\sigma_E/E = [1.3 \oplus (0.07/E) \oplus (0.8/E^{1/4})]\%$, ($E$ in GeV). Neutral pions are detected via their $\pi^0 \to \gamma\gamma$ decay. The π^0 mass resolution varies slowly with energy, averaging $\sigma_{m_{\pi^0}} = 4.9$ MeV. For a $\pm 3\sigma$ mass selection requirement, the overall detection efficiency for π^0's from $B\overline{B}$ events (including the effects of geometrical acceptance) is 40%.

Electron identification in Belle is based on a combination of dE/dx measurements in the CDC, the response of the ACC, and the position, shape and total energy (i.e. E/p) of its associated CsI shower. The electron identification efficiency is determined from two-photon $e^+e^- \to e^+e^-e^+e^-$ processes to be more than 90% efficient for $p_{lab} > 1.0$ GeV detected tracks and the hadron misidentification probability, determined using tagged pions from inclusive $K^0 \to \pi^+\pi^-$ decays, is below 0.5%.

The 1.5 Tesla magnetic field is returned via an iron yoke that is instrumented to detect muons and K_L mesons. This detection system, called the KLM, consists of alternating layers of charged particle detectors and 4.7 cm thick steel plates [8]. The total steel thickness of 65.8 cm plus the material of the inner detector corresponds to 4.7 nuclear interaction lengths at normal incidence. The system covers laboratory polar angles between $\theta = 20^o$ and 155^o and the overall muon identification efficiency, determined by embedding tracks from $e^+e^- \to e^+e^-\mu^+\mu^-$ events into real multihadron events, is greater than 90% for $p_{lab} > 1$ GeV tracks detected in the inner tracker. The corresponding pion misidentification probability, determined using $K^0 \to \pi^+\pi^-$ decays, is less than 2%.

III. EVENT SELECTION

We concentrate on three final state topologies:

$$B^+ \to J/\psi K^+\pi^+\pi^-,$$
$$B^0 \to J/\psi K^+\pi^-\pi^0,$$
$$B^0 \to J/\psi K^0\pi^+\pi^-.$$

(Here, as in the rest of this report, the inclusion of the charge conjugate states is always implied.) In all cases we require that the J/ψ decays via $J/\psi \to \ell^+\ell^-$. We apply the same J/ψ and charged kaon selection criteria to the same data sample to extract a large sample of $B^+ \to J/\psi K^+$ decays for normalization.

For $J/\psi \to \mu^+\mu^-$ candidates we use oppositely charged track pairs where at least one track is positively identified as a muon by the KLM system and the other is either positively identified as a muon or has a CsI energy deposit that is consistent with a minimum ionizing

particle. The invariant mass of the candidate $\mu^+\mu^-$ pair is required to be within $\pm 3\sigma$ (± 33 MeV) of the J/ψ mass peak.

Candidate $J/\psi \to e^+e^-$ decays are oppositely charged track pairs where at least one track is well identified as an electron and the other track satisfies at least the dE/dx or the CsI E/p electron identification requirements. In this channel, we partially correct for final state radiation or real bremsstrahlung in the inner parts of the detector by including the four-momentum of every photon detected within 0.05 radians of the original electron direction in the e^+e^- invariant mass calculation. Since the $J/\psi \to e^+e^-$ peak still has a small radiative tail, we use an asymmetric invariant mass requirement $6\sigma \leq (M_{e^+e^-} - M_{J/\psi}) \leq 3\sigma$, where $\sigma = 13$ MeV.

For charged kaon candidate tracks we require a minimum level of positive kaon identification. For $K^0 \to \pi^+\pi^-$, we use opposite charged track pairs where the displacement of the $\pi^+\pi^-$ vertex from the interaction region in the transverse $(r-\phi)$ plane is more than 1 mm, the ϕ coordinate of the $\pi^+\pi^-$ vertex point and the ϕ direction of the $\pi^+\pi^-$ candidate's three momentum vector agree within 0.2 radians, and $|M_{\pi^+\pi^-} - M_{K^0}| \leq 12$ MeV.

For charged pions, we reduce multiple entries from the same event by only using tracks that are not identified as a charged kaon, have $p_{lab} > 0.2$ GeV and have at least 20 associated CDC hits. For the $J/\psi K^+\pi^+\pi^-$ mode we require $|M_{\pi^+\pi^-\ell^+\ell^-} - M_{\ell^+\ell^-} - 0.59\text{GeV}| > 0.009$ GeV. This eliminates $B^+ \to \psi(2s)K^+$ decays where $\psi(2s) \to \pi^+\pi^- J/\psi$. For π^0 candidates we use pairs of γ's with an invariant mass within $\pm 3\sigma$ of M_{π^0}. To reduce multiple entries, we only use γ's with $E_{lab} > 50$ MeV and π^0's with $p_{lab} > 400$ MeV. Monte Carlo studies indicate that with these cuts the level of multiple entries is below 5% for the $K^+\pi^+\pi^-$ and 10% for the $K^+\pi^-\pi^0$ channels.

IV. SIGNAL YIELD

Figure 1a shows a scatterplot of energy difference, ΔE, *vs* beam constrained mass, M_b, for all selected events, where

$$\Delta E \equiv \sum_{i=1,n} E_i - E_{cm}/2, \tag{1}$$

and

$$M_b \equiv \sqrt{\left(\frac{E_{cm}}{2}\right)^2 - \left(\sum_{i=1,n} \vec{p}_i\right)^2}. \tag{2}$$

Here E_{cm} is the cm energy of the colliding e^+ and e^-, and $\vec{p}_i$ and E_i are the three momentum and total energy of each of the n B meson decay products evaluated in the e^+e^- cm frame. The $B \to J/\psi K\pi\pi$ signal region in Fig. 1a is indicated by a solid-line rectangle of sides $\pm 3\sigma$ around $M_b = 5.28$ GeV and $\Delta E = 0$. An equal-area sideband region centered at $\Delta E = 0.12$ GeV is indicated by dashed lines [9]. The clear histogram in Fig. 1b shows the M_b projection for the ΔE signal region; the shaded histogram shows the same for the sideband ΔE region. There is some excess in the signal histogram near $M_b = 5.28$ GeV, but the background, as indicated by the sideband histogram, is substantial.

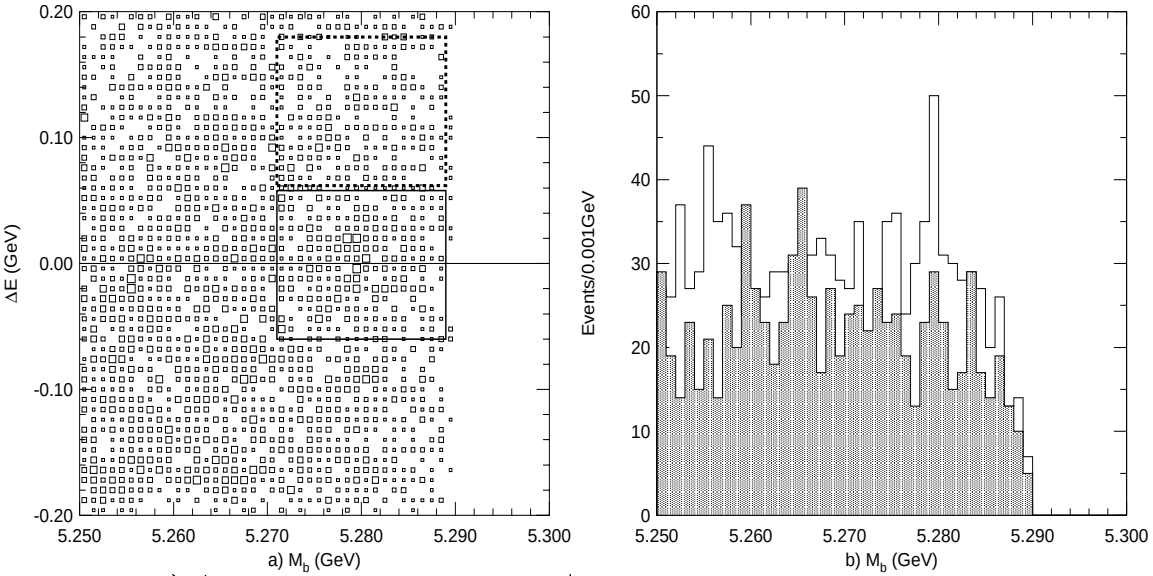

FIG. 1. **a)** ΔE *vs* M_b for the selected $J/\psi K\pi\pi$ events. The $\pm 3\sigma$ signal and sideband regions are indicated by the solid and dashed rectangles. **b)** The M_b projections for events in the ΔE signal (clear) and sideband (shaded) regions.

Figures 2a and b show scatter plots of $M_{\pi\pi}$ (vertical) *vs* $M_{K\pi\pi}$ for events in the ΔE *vs* M_b sideband and signal regions of Fig. 1. The signal region data (Fig. 2b) has a strong clustering of events in the region near $M_{\pi\pi} \sim 0.75$ GeV and $M_{K\pi\pi} \sim 1.3$ GeV that is not evident in the sideband data. This cluster is what is expected for $K\pi\pi$ systems that originate from the decay of the $K_1(1270)$ resonance.

The PDG world average $K_1(1270)$ mass is $M_{K_1} = 1.273 \pm 0.007$ MeV and width is , $_{K_1} = 90 \pm 20$ MeV; its most prominent decay mode is $K_1(1270) \to K\rho$ (Br= 42%) [10]. Since the peak mass is very nearly equal to $M_\rho^{peak} + M_K$, events corresponding to $K_1 \to K\rho$, $\rho \to \pi\pi$ populate a region near the kinematic boundary in Fig. 2b. Both the K_1 and ρ line shapes are distorted by threshold effects; the K_1 preferentially decays into lower mass ρ mesons. For this reason we make a $M_{\pi\pi}$ selection requirement that is asymmetric around M_ρ^{peak}, namely $0.62 \leq M_{\pi\pi} \leq 0.84$ GeV, as indicated by the horizontal dashed lines in Figs. 2a and b.

Figures 2c and d show the sideband and signal region $M_{K\pi\pi}$ distributions for events where $M_{\pi\pi}$ is in the ρ mass region. The curve in Fig. 2c shows the result of a fit to a phase-space-like background function to the sideband $M_{K\pi\pi}$ distribution. The curve in Fig. 2d shows the results of a fit that uses the background determined from the sideband distribution plus a line shape function that was specialized to expectations for $K_1 \to K\rho$ decays and uses the PDG values for the K_1 mass and total width [11]. The sideband background plus the K_1 line shape function, which has only its normalization as a free parameter, gives a good fit to the low mass region of the signal region $K\pi\pi$ mass spectrum, indicating that our interpretation of the event cluster in Fig. 2b as being due to the $K_1(1270)$ is reasonable. (The validity of this interpretation is discussed below in Section VI.) For subsequent analysis we select $K_1(1270)$ events as those that satisfy the ρ mass requirements and have with $M_{K\pi\pi} \leq 1.38$ GeV. The MC simulation indicates that this mass window accepts 41% of all $K_1(1270) \to K\pi\pi$ decays.

Figure 3a shows the ΔE vs M_b distribution for all of the $B \to J/\psi K\pi\pi$ event candidates

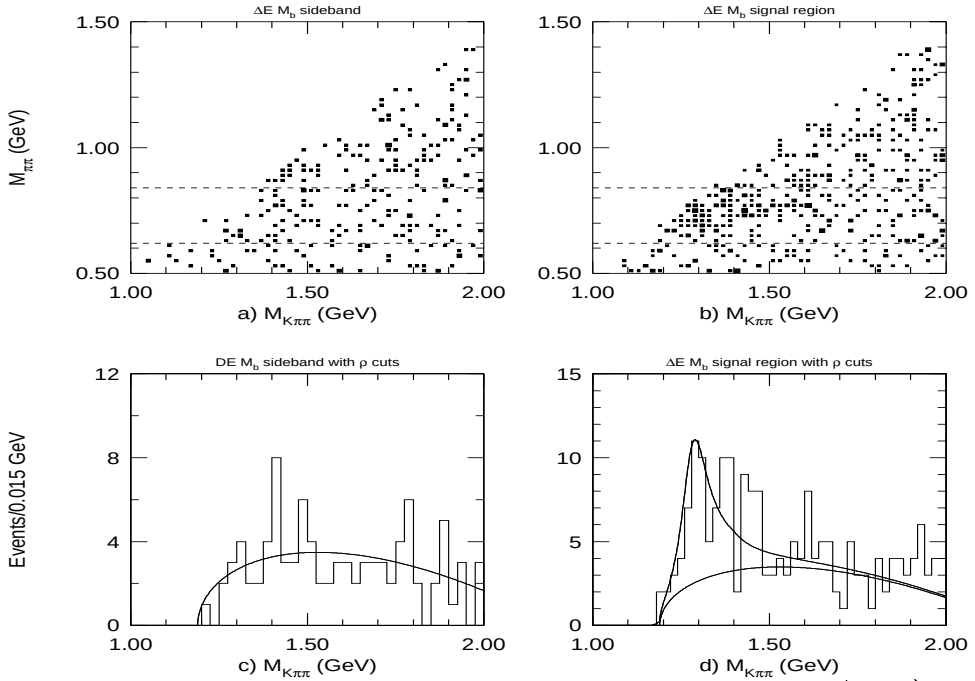

FIG. 2. The distribution of $M_{\pi\pi}$ *vs* $M_{K\pi\pi}$ for events in the M_B and ΔE **a)** sideband and **b)**signal region. The $M_{K\pi\pi}$ distributions for the events with $0.62 \leq M_{\pi\pi} \leq 0.84$ GeV for the **c)** sideband and **d)** signal regions. The curves represent fits that are described in the text.

after the application of the $K_1(1270)$ mass requirements. The rectangle denotes the $\pm 3\sigma$ signal region for B meson decay. Here a prominent signal is evident above a relatively small background level. Figures 3b, c and d, show the individual distributions for the $K^+\pi^+\pi^-$, $K^+\pi^-\pi^0$ and $K^0\pi^+\pi^-$ channels, respectively [12].

Figures 4a through h show, alternatively, the projections of the M_b and ΔE signal bands for: all channels combined (a and b), the $J/\psi K^+\pi^+\pi^-$ mode (c and d), the $J/\psi K^+\pi^-\pi^0$ mode (e and f), and the $J/\psi K^0\pi^+\pi^-$ mode (g and h). (Specifically, the left-hand panels in Fig. 4 show the M_b distribution for events with $|\Delta E| < 0.06$ GeV and the right-hand panels the ΔE distribution for events with $|M_b - 5.28| < 0.009$ GeV.) The curve in each figure is the result of a simultaneous fit to the M_b and ΔE projections where the two distributions are fit with Gaussian signal functions that are constrained to have the same number of events. For the M_b projection, we parameterize the background with a function that has a phase-space-like behavior near the endpoint [13]; for ΔE, we represent the background with a second-order polynomial. For the fits to the combined channel distributions (Figs. 4a and b) and the $K^+\pi^+\pi^-$ channel (Figs. 4c and d), the values of the signal peaks and widths are free parameters; the fit results are consistent with MC expectations. In the $K^+\pi^-\pi^0$ and $K^0\pi^+\pi^-$ channels, where the statistics are limited, the signal peak positions and widths are fixed at their expected values.

We use the $B^+ \to J/\psi K^+$ events from the same data sample for normalization. We select these events using the same J/ψ and charged kaon criteria as used in the $B \to K\pi\pi$ selection and find a distinct signal with very little background. The results of the fits for all channels are listed in Table I.

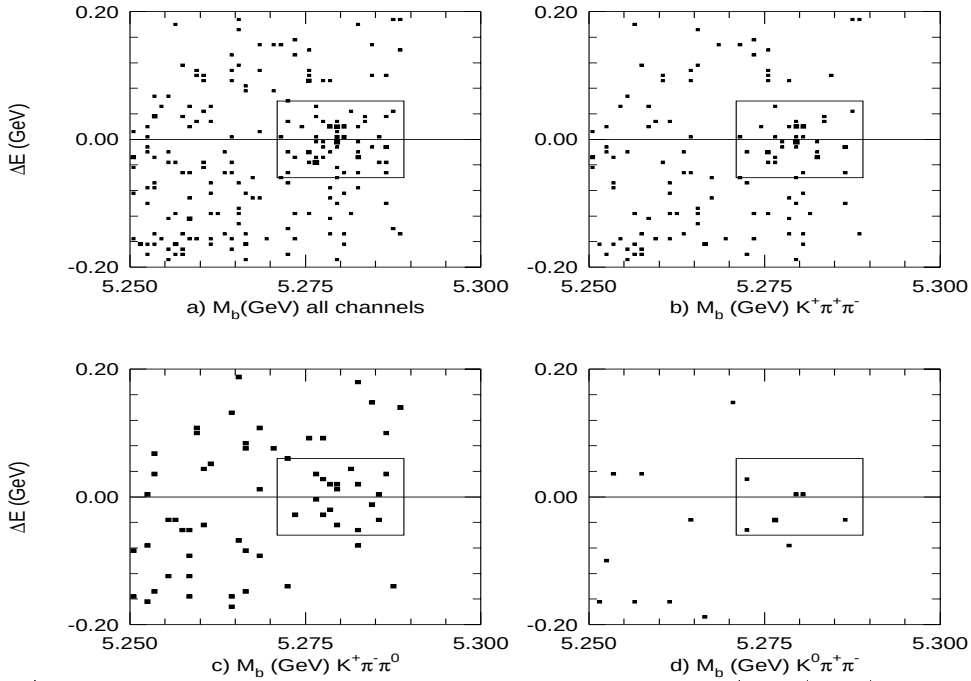

FIG. 3. **a)** The distribution of ΔE *vs* M_b for all selected $B \to J/\psi K_1(1270)$ candidate events. The $K^+\pi^+\pi^-$, $K^+\pi^-\pi^0$ and $K^0\pi^+\pi^-$ channels are shown separately in **b), c)** and **d)**, respectively.

TABLE I. Results of the fits to the M_b and ΔE projections.

Channel	N_{evts}
$J/\psi K\pi\pi$ (all channels combined)	$45.0^{+8.7}_{-8.3}$
$J/\psi K^+\pi^+\pi^-$	$25.2^{+6.7}_{-6.3}$
$J/\psi K^+\pi^-\pi^0$	$12.9^{+4.6}_{-4.1}$
$J/\psi K^0\pi^+\pi^-$	$4.9^{+2.7}_{-2.3}$
$J/\psi K^+$	238.0 ± 15.9

V. BRANCHING FRACTION RESULTS

We determine the ratio of branching fractions from the relation

$$\frac{\mathcal{B}(B \to J/\psi K_1)}{\mathcal{B}(B^+ \to J/\psi K^+)} = \frac{N_{evt}^{J/\psi K_1}\ \eta_{J/\psi K^+}\ f_i}{N_{evt}^{J/\psi K^+}\ \eta_{J/\psi K_1}}, \tag{3}$$

where η denotes the Monte-Carlo determined acceptances for each process. For the charged mode, $f_i = 1$; for the neutral mode $f_i = f_+/f_0$ $(= 1.07 \pm 0.09)$, the ratio of charged to neutral B meson production at the $\Upsilon(4S)$ [14].

The results for the two neutral K_1^0 modes are

$$\frac{\mathcal{B}(B^0 \to J/\psi K_1^0(1270))}{\mathcal{B}(B^+ \to J/\psi K^+)} = 1.2 \pm 0.5 \qquad (K^+\pi^-\pi^0 \text{ mode})$$

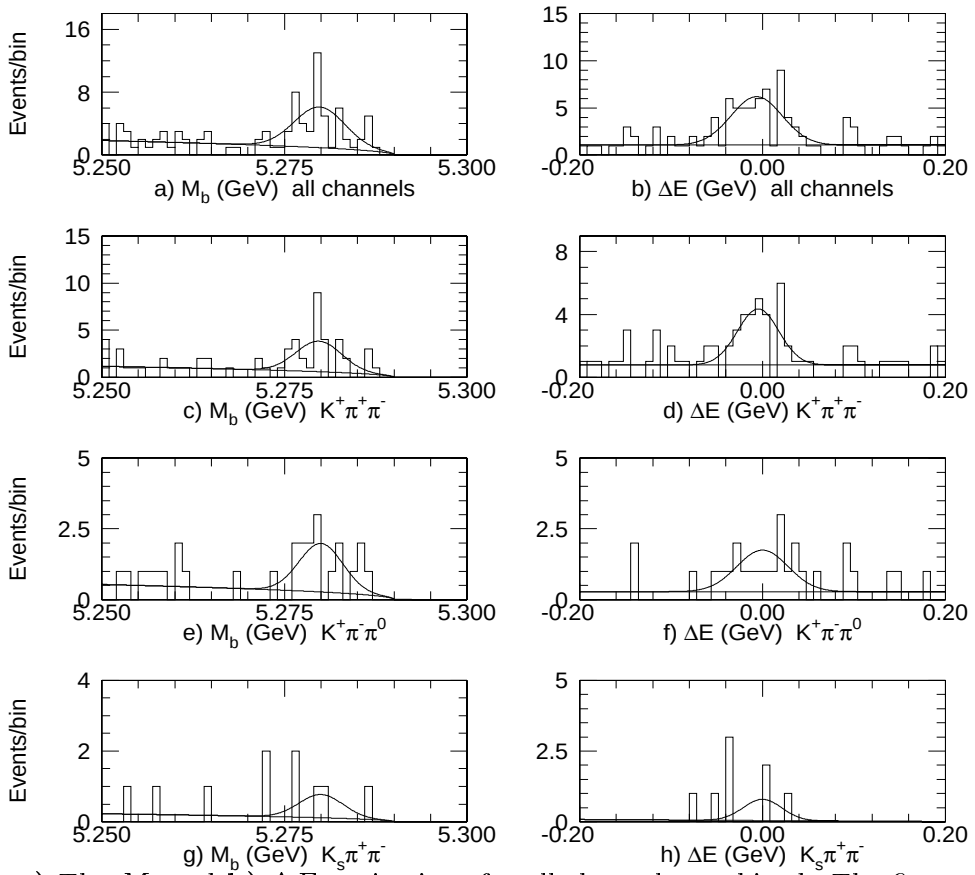

FIG. 4. **a)** The M_b and **b)** ΔE projections for all channels combined. The fits are described in the text. The corresponding distributions and fits for the individual $K^+\pi^+\pi^-$, $K^+\pi^-\pi^0$, and $K^0\pi^+\pi^-$ channels are also shown.

$$\frac{\mathcal{B}(B^0 \to J/\psi K_1^0(1270))}{\mathcal{B}(B^+ \to J/\psi K^+)} = 2.7^{+1.5}_{-1.3} \qquad (K^0\pi^+\pi^- \text{ mode}),$$

where only statistical errors are shown [15]. Since the results for the two modes are consistent within errors, we combine the two measurements. The branching fraction results are:

$$\frac{\mathcal{B}(B^0 \to J/\psi K_1^0(1270))}{\mathcal{B}(B^+ \to J/\psi K^+)} = 1.4 \pm 0.4 \pm 0.4$$
$$\frac{\mathcal{B}(B^+ \to J/\psi K_1^+(1270))}{\mathcal{B}(B^+ \to J/\psi K^+)} = 1.5 \pm 0.4 \pm 0.3,$$

where the second quoted errors are systematic and are discussed below in Section VII. These results are preliminary. Final results based on all of the currently available data and with a more complete study of systematic errors will be available in the near future.

VI. NON-$K_1(1270)$ SIGNAL COMPONENTS.

We examined the possibility of contributions from sources other than the $K_1(1270)$ to the observed signal. We considered two possibilities: other resonances and non-resonant $K\pi\pi$ production.

There are two resonances that overlap the $K_1(1270)$ and decay to $K\pi\pi$ final states, the $K_1(1400)$ and $K^*(1410)$, both of which primarily decay to $K^*(890)\pi$. Although neither of these resonances has an appreciable $K\rho$ branching fraction, the limited phase space available in the decay results in about one third of $K^*\pi$ final states producing two pions that satisfy the $M_{\pi\pi}$ requirements. A separate search for $B \to J/\psi K^*(890)\pi$ decays using selection criteria optimized for this channel [16] did not uncover a significant signal for either of these states and indicated that the level of contribution from these higher mass states to the observed signal is $(3 \pm 10)\%$.

The $K_1(1270)$ yield in our $\pi\pi$ and $K\pi\pi$ mass window, determined from fitting the signal region $M_{K\pi\pi}$ distribution using a background determined from the ΔE-M_b sideband region (shown in Fig. 2d), 42.6 ± 8.1 events, agrees, within 10%, with the number of signal events determined from the simultaneous fits to the ΔE and M_b projections shown in Figs. 4a and b. This indicates that the non-resonant part of the $M_{K\pi\pi}$ spectrum constitutes most of the background in the ΔE-M_b projections and rules out a substantial non-resonant $K\pi\pi$ component to our observed signal.

We also applied the same selection process to a large sample of inclusive $B \to J/\psi X$ Monte Carlo events, which includes some non-resonant $J/\psi K\pi\pi$ decays generated with a phase space $M_{K\pi\pi}$ distribution. The selected events have no peak near the $K_1(1270)$; if we fit for a resonance, we get a yield that is slightly negative and consistent with zero. This is evidence that our analysis method does not manufacture a peak.

VII. SYSTEMATIC ERRORS

The main systematic errors and estimates of their magnitude are listed in Table II. The largest systematic errors are due to uncertainties in the $K_1(1270)$ branching fractions to the $K\pi\pi$ states that are accepted. We also include in the systematic error the uncertainties associated with possible contributions to the signal from sources other than the $K_1(1270)$. A source of error for the neutral mode is the experimental uncertainty in f_+/f_0.

TABLE II. Sources of systematic errors.

Error source	$K_1^+(1270)$	$K_1^0(1270)$
$K_1(1270)$ branching fractions	14%	14%
other $K\pi\pi$ resonance	13%	13%
non-resonant $K\pi\pi$	10%	10%
f_+/f_0 (neutral mode only)	-	8%
$\pi^+\pi^{-(0)}$ data/MC differences	5%	10%
Quadrature sum	22%	25%

By quoting our results as a ratio of branching fractions, many experimental systematic effects tend to cancel out. These include effects due to uncertainties in the number of B mesons, and the J/ψ and charged kaon detection and identification efficiencies. The major remaining experimental systematic error is the efficiency for low momentum charged

and neutral pion and neutral kaon detection, where we rely on the results of Monte Carlo simulation. Agreement between data and MC simulation results for various calibration processes has been demonstrated at the $\sim 5\%$ level for charged pions and $\sim 10\%$ level for neutral pions and kaons [17]. These uncertainties are included in the systematic error.

VIII. DISCUSSION

We observe that the $K_1(1270)$ is a dominant component of $B \to J/\psi K\pi\pi$ decays. This is of special interest for CP violation studies because among the low mass resonances, the $K_1^0(1270)$ has the largest branching fraction for decays to the *flavor-nonspecific* $K^0\rho^0$ final state. In principle, these final states are mixtures of CP=± 1 eigenstates, depending on the orbital angular momentum of the J/ψ and the K_1. With sufficient statistics, the relative strengths of the two CP eigenstates can be determined from an analysis of final state helicity angle distributions [18]. This is similar to the situation for the much discussed flavor-nonspecific $B^0 \to J/\psi K^{*0} \to J/\psi K^0\pi^0$ decay channel. However, the $J/\psi K^0\pi^+\pi^-$ case is made more complicated by the different intermediate states that can be present. In addition to the $K^0\rho$ intermediate state, there are also contributions from the *flavor-specific* $K^*\pi$ and $K_0^*(1430)\pi$ channels. Theoretical work is needed to clarify the situation.

IX. SUMMARY

We report the first observation of decays of the type $B \to K_1(1270)J/\psi$ and report preliminary values for branching fraction ratios relative to that for $B^+ \to J/\psi K^+$. Using the PDG value of $\mathcal{B}(B^+ \to J/\psi K^+) = (9.9 \pm 1.0) \times 10^{-4}$ [10], we translate our results to

$$\mathcal{B}(B^0 \to J/\psi K_1^0(1270)) = (1.4 \pm 0.4 \pm 0.4) \times 10^{-3}$$
$$\mathcal{B}(B^+ \to J/\psi K_1^+(1270)) = (1.5 \pm 0.4 \pm 0.4) \times 10^{-3}.$$

These modes constitute a reasonable portion ($\sim 15\%$) of the total number of $B \to J/\psi X$ decays.

We observe ~ 4 events with a background level of ~ 1 event for the flavor-nonspecific channel $B \to J/\psi K_1^0 \to J/\psi K^0\pi^+\pi^-$. Here two possible CP states are accessible. More data will permit a determination of their relative contributions.

X. ACKNOWLEDGEMENTS

We gratefully acknowledge the efforts of the KEKB group in providing us with excellent luminosity and running conditions and the help with our computing and network systems provided by members of the KEK computing research center. We thank the staffs of KEK and collaborating institutions for their contributions to this work, and acknowledge support from the Ministry of Education, Science, Sports and Culture of Japan and the Japan Society for the Promotion of Science; the Australian Research Council and the Australian Department of Industry, Science and Resources; the Department of Science and Technology of India; the BK21 program of the Ministry of Education of Korea and the Basic Science

program of the Korea Science and Engineering Foundation; the Polish State Committee for Scientific Research under contract No.2P03B 17017; the Ministry of Science and Technology of Russian Federation; the National Science Council and the Ministry of Education of Taiwan; the Japan-Taiwan Cooperative Program of the Interchange Association; and the U.S. Department of Energy.

REFERENCES

[1] D. Bortoletto *et al.* (CLEO), Phys. Rev. **D45**, 21 (1992) and H. Albrecht *et al.* (Argus), Phys. Lett. **B199**, 451 (1987). Both of these papers quote branching fractions for $B^+ \to J/\psi K^+\pi^+\pi^-$ based on $3 \sim 5$ signal events.

[2] See, for example, Y. Funakoshi *et al.*, *KEKB Performance*, Proc. 2000 European Particle Accelerator Conference, Vienna(2000), and references cited therein.

[3] G. Alimonti *et al.* , *The BELLE silicon vertex detector*, KEK preprint 2000-34 (2000), submitted for publication in Nucl. Instr. Meth. **A**.

[4] H. Hirano *et al.*, *A high resolution cylindrical drift chamber for the KEK B-factory*, KEK Preprint 2000-2 and M. Akatsu *et al.*, *Cathode image readout in the BELLE CDC*, Nagoya Univ. preprint DPNU-00-06; both papers have been accepted for publication in Nucl. Instr. Meth. **A**.

[5] H. Kichimi *et al.*, *The Belle TOF system*, Proceedings of the 7th International Conference on Instrumentation for Colliding Beam Physics, Hamamatsu, Japan, Nov. 15-19, 1999.

[6] T. Iijima *et al.*, *Aerogel Cherenkov counter for the Belle detector*, Proceedings of the 7th International Conference on Instrumentation for Colliding Beam Physics, Hamamatsu, Japan, Nov. 15-19, 1999.

[7] H. Ikeda *et al.* , Nucl. Instr. Meth. **A441**, 401 (2000).

[8] A. Abashian *et al.* ,Nucl. Instr. Meth. **A449**, 112 (2000).

[9] The $B \to J/\psi K3\pi$ process, where one low energy pion is missed, would populate the $M_b \sim 0$ and negative ΔE region. Therefore, we do not use the negative ΔE region for sideband studies.

[10] C. Caso *et al.* (PDG), Eur. Phys. J. **C3**, 1 (1998).

[11] W. M. Dunwoodie, private communication. See also, J.Z. Bai *et al.* (BES), Phys. Rev. Lett. **83**, 1918 (1999).

[12] Only one selected event in the signal region has multiple entries (in the $K^+\pi^+\pi^-$ channel). In the plots we only include the entry with an $M_{\pi^+\pi^-}$ value that is closest to M_ρ.

[13] This function has the form $f(x) = Ax\sqrt{1-4(x/E_{cm})^2}exp(1-4(x/E_{cm})^2)$.

[14] J.P. Alexander *et al.* CLEO, *Measurement of the Relative Branching Fraction of* $\Upsilon(4S)$ *to Charged and Neutral B-Meson Pairs*, hep-ex/0006002, Submitted to Phys. Rev. Lett.

[15] Statistical errors include the errors on the numbers of signal and $J/\psi K^+$ events from the fits and the MC-statistics component of the acceptance error added in quadrature.

[16] The replacement of the $M_{\pi\pi}$ selection with the requirement $|M_{K\pi} - M_{K^*}| < 0.075$ GeV enhances the efficiency for $K^*\pi$ decays by a factor of 2.6.

[17] For example, we evaluate the $\pi^+\pi^-$ tracking efficiency from a comparison of data and MC results for the ratio $N(D^0 \to K^-\pi^+\pi^+\pi^-)/N(D^0 \to K^-\pi^+)$, and the π^0 and K^0 detection efficiencies from $N(D^0 \to K^-\pi^+\pi^0)/N(D^0 \to K^-\pi^+)$ and $N(D^0 \to K^0\pi^+\pi^-)/N(D^0 \to K^-\pi^+)$.

[18] See, for example, I. Dunietz, H. Quinn, A. Snyder, W. Toki, and H.J. Lipkin, Phys. Rev. **D43**, 2193 (1991).